

## A NOVEL STUDY BASED ON ADAPTIVE SOLITARY PULMONARY NODULE SEGMENTATION USING DIGITAL RADIOGRAPHY IMAGES

J. Vijayaraj<sup>1</sup>, Dr. D. Loganathan<sup>2</sup>

<sup>1</sup>Ph.D. Scholar, <sup>2</sup>Professor, Department of CSE, PEC, Puducherry India

**ABSTRACT**— In Digital Radiography (DR) images often have uncertain contours and infiltration, which make it a stimulating task for outdated segmentation models to get satisfactory segmentation results. To overwhelm this, this paper has suggested an adaptive SPN segmentation model for DR images based on random walks segmentation and sequential filter. At First, the SPN image is disintegrated to get the animated component which is recycled to obtain a set of seeds. Secondly, the seeds selection tactic is laboring to enhance the scope of walking pixels and decrease the number of seeds, which could decrease the computational price. Lastly, we join the sequential filter and construct the novel demonstration of the weight and the probability matrices. This paper is about to analyze the various Pulmonary modules in the cancer segmentation which is being implemented in MATLAB. The comparison of DR and CT images is being surveyed in this work

**Index Terms**— CT Image, Image segmentation, Sequential filter, Digital Radiography, Solitary Pulmonary Nodule.

### INTRODUCTION

Lung cancer ranks first in the death of malignant tumor as reported by the World Health Organization. Therefore, early detection and treatment are important to reduce the mortality of lung cancer. Solitary Pulmonary Nodule (SPN) is one of the important characteristic of early lung cancer. The location, the size and the rate of the growth are important indicators for diagnosis. The accuracy of SPN segmentation is essential to judge the real condition. The correct segmentation results are the premise of feature extraction and character analysis [1]. Due to unique noise characteristics in medical images we do not have common techniques suitable for all segmentation problems.

Lung cancer screening programs with low-dose CT imaging are being implemented in the US. Currently, only 15% of all diagnosed lung cancers are detected at an early stage, which causes a five-year survival rate of only 16%. The aim of screening is to detect cancers in an

earlier stage when curative treatment options are better [2].

Unlike CT images, DR images lack of tomography information. It is represented as just one image. In general, the center of the SPN is characterized as high brightness, and tissues near the margin of the lesion often show as fuzzy thin shadow. In most images, the edges of SPN are blurred even missing. The fuzzy clustering method is widely employed in medical image processing. Too many improvements have been made to adapt to lesion segmentation. The lung parenchyma is divided into several clusters, and different processing methods were constructed to get the region of Interest. Claus' clustering algorithm can handle the vessel, crossing point and the solitary nodule. But it mainly focuses.

On detecting nodules for CAD systems, and does not care other features. Besides, the complex clustering brings much time consumption.

Although it has been shown that CAD systems improve the reading efficiency of radiologists, a considerable number of nodules remains undetected at low false positive rates, Prohibiting the use of CAD in clinical illustrates that nodules come with a wide variation in shapes, sizes, and types (e.g., solid, sub solid, calcified, pleural, etc.). In addition, the number of nodules from different categories are highly imbalanced and many irregular lesions that are visible in CT are not nodules. As a consequence, extracting underlying characteristics of nodules is difficult and requires many heuristic steps [3]. Techniques to detect lesions with a broad spectrum of appearances are needed to improve the performance of CAD systems.

In this paper, we analyze the structure of the DR pulmonary nodules, and present an improved adaptive random walks segmentation which integrates sequential filter. Firstly, the original SPN image is decomposed into texture and cartoon components which is used to get the seeds. Secondly, based on the seeds, the walker pixels and seeds selection tactic are employed to reduce the computational overhead [4]. Then, we incorporate the

sequential filter to random walks, and define the improved weight representation and probability matrices. Finally, the proposed method is exploited to get the segmentation results. The proposed method has the properties as below:

1. The fast seeds acquisition method that is based on the cartoon component could fast and effectively get the seeds without iteration.
2. Seeds selection tactic optimally selects the walking pixels and reduce the number of seeds [5] [6] [7]. This tactic could avoid contour leaking and reduce computational cost at the same time.
3. Its combination with the sequential filter could smooth the inhomogeneous region and avoid over-smoothing. The newly defined weight representation and probability matrices could improve the segmentation [9].
4. The proposed method could ensure the precise segmentation results even the image definition is poor.

## 1. LITERATURE SURVEY

**1.1 Title:** CT screening for lung cancer: Is the evidence strong enough?

**Author:** Field JK, Devaraj A, Duffy SW, Baldwin DR.

### ABSTRACT:

The prevailing questions at this time in both the public mind and the clinical establishment is, do we have sufficient evidence to implement lung cancer Computed Tomography (CT) screening in Europe? If not, what is outstanding? This review addresses the twelve major areas, which are critical to any decision to implement CT screening and where we need to assess whether we have sufficient evidence to proceed to a recommendation for implementation in Europe [10]. The readiness level of these twelve categories in 2015 have been with color coded, where green indicates we have sufficient evidence, amber is borderline evidence and red requires further evidence. Recruitment from the 'Hard to Reach' community still remains at red, while mortality data, cost effectiveness and screening interval are all categorized as amber. The integration of smoking cessation into CT screening programmes is still considered to be category amber. The US Preventive Services Task Force have recommended that CT screening is implemented in the USA utilizing the NLST criteria, apart from continuing screening to 80 years of age. The cost effectiveness of the NLST was calculated to be \$81,000/QALY, however, it's well-recognized that the costs of medical care in the USA, is far higher than that of Europe. Medicare have agreed to cover the cost of screening but

have stipulated a number of stringent requirements for inclusion. To date we do not have good CT screening mortality data available in Europe and eagerly await the publication of the NELSON trial data in 2016 and then the pooled UKLS and NELSON data thereafter. However in the meantime we should start planning for implementation in Europe, especially in the areas of the radiological service provision and accreditation, as well as identifying novel mechanisms to recruit from the hardest to reach communities.

**1.2 Title:** An adaptive window mechanism for image smoothing

**Author:** Ardeshir Goshtasbya, Martin Satterb

### ABSTRACT:

Image smoothing using adaptive windows whose shapes, sizes, and orientations vary with image structure is described. Window size is increased with decreasing gradient magnitude, and window shape and orientation are adjusted in such a way as to smooth most in the direction of least gradient. Rather than performing smoothing isotopically, smoothing is performed in preferred orientations to preserve region boundaries while reducing random noise within regions. Also, instead of performing smoothing uniformly, smoothing is performed more in homogeneous areas than in detailed areas. The proposed adaptive window mechanism is tested in the context of median, mean, and Gaussian filtering, and experimental results are presented using synthetic and real images and compared with a state-of-the-art method [12].

**1.3 Title:** Comparative study of DR and CT in the application of close contacts screening for tuberculosis outbreaks

**Author:** XiweiLu, XuemeiWang, DaLia, JianlinWub

### ABSTRACT:

**Objective:** To assess the value of direct digital radiography (DR) and CT in the screening of tuberculosis. **Methods:** In a tuberculosis outbreak in May, 2014, both chest DR and CT were taken in the close contacts. The chi square test and ROC curve were used to evaluate and calculate the missed pulmonary lesions from DR and the natures of these lesions. **Results:** Abnormal shadow detection rates of chest DR and CT were 22.9% (8/35) and 40% (14/35) respectively, the difference was statistically significant ( $\chi^2$  &61; 16.154, P &60; 0.01). In the 6 missed cases from chest DR, 3 cases showed with anatomical occult or overlap, such as local area between azygos vein and

esophagus (1 case), lung markings in the lower lobe and diaphragmatic occlusion and in the other 3 missed cases, early signs of small nodules or tree-in-bud were the major signs. ROC analysis showed that when the axis of tree-in-bud is less than 22 mm, it was prone to produce misdiagnosis by using the chest DR. The area under the ROC curve (AUC) was 0.925 with the sensitivity of 90% and specificity of 83.3%. In the 14 cases detected on CT, the lung was involved in 12 cases and the pleura was involved in 2 cases. For the 12 lung-involved cases, the lesions involving from one lung segment to five lung segments were occurred in 6 cases (50.0%), 2 cases (16.7%), 1 case (8.3%), 1 case (8.3%), and 2 cases (16.7%), respectively. Tree-in-bud signs were the main CT characteristics in close contacts, and accounted for about 91.7% (11/12). All the 4 pleura-involved cases showed pleural thickening and pleural tuber culoma after 3–4 months' anti-TB therapy. In the 14 cases detected by CT, 6 cases with micro-lesions were taken by anti-TB experimental treatment, only 2 cases was significantly absorbed of the lesions after 2 months, and all the lesions of the 6 cases absorbed after 6 months anti-TB treatment. Conclusion; CT is more valuable in the screen of TB outbreak in school compared with DR. Subclinical cases detected by CT is recommended to take a formal anti-TB treatment[11].

## 2. SEGMENTATION OF SOLITARY PULMONARY NODULE

A solitary pulmonary nodule (SPN) or coin lesion is a mass in the lung smaller than 3 centimeters in diameter. It can be an incidental finding found in up to 0.2% of chest X-rays and around 1% of CT scans.

The nodule most commonly represents a benign tumor such as a granuloma or hamartoma, but in around 20% of cases it represents malignant cancer especially in older adults and smokers. Conversely, 10 to 20% of patients with lung cancer are diagnosed in this way. If the patient has a history of smoking or the nodule is growing the possibility of cancer may need to be excluded through further radiological studies and interventions, possibly including surgical resection. The prognosis depends on the underlying condition [13].

### Definition

Nodular density is used to distinguished larger lung tumors, smaller infiltrates or masses with other accompanying characteristics. An often used formal radiological definition is the following: a single lesion in the lung completely surrounded by lung parenchyma (functional tissue) with a diameter less than 3 cm

and without associated pneumonia, atelectasis or lymphadenopathies.

### Methods

Two main stages are incorporated: 1) candidate's detection and 2) false positive reduction. We applied three candidates detectors specifically designed for solid, sub solid, and large solid nodules. The combination of these detectors is applied to increase the detection sensitivity of nodules. Note that nodules have a large variations in both size and morphological characteristics. For each candidate, we extract multiple 2-D views in fixed planes. Each 2-D view is then processed by one ConvNets stream. The ConvNets features are then used to compute a final score. In the next sections we describe the CAD system in details.

#### 2.1 Candidates Detection

Candidate detection algorithms play an important role in the performance of any CAD system, as it determines the maximum detection sensitivity of subsequent stages. Candidate detection algorithms should ideally detect all suspicious lesions. However, the morphological variation of nodules is often greater than what a single candidate detection algorithm can detect [15]. To detect a wider spectrum of nodules, we applied a combination of multiple algorithms used for candidate detection. Three existing CAD systems are used to detect nodule candidates. Each algorithm aims at a specific type of nodules, namely solid nodules, sub solid nodules, and large solid nodules. For each candidate, the position and the nodule probability are given. Three sets of nodule candidates are computed and are merged in order to maximize the sensitivity of the detector. The candidates located closer than 5 mm to each others are merged. For these combined candidates, the position and nodule probability are averaged. The methods for candidate detection stage, for which the locations of volume of interest (VOI) are obtained.

#### 2.2 Patches Extraction

For each candidate, we extracted multiple 2-D patches of 50 50 mm the size of the patch was chosen in order to have all nodules ( $\leq 30$ mm) fully visible on the 2-D views and include sufficient context information to aid in the classification of the candidate. We resized each 50X50 mm patch to a size of 64X64 px, working at the resolution of 0.78 mm, which corresponds to the typical resolution of thin slice CT data. The pixel intensity range is rescaled from (-1000, 400 HU) to (0, 1). Intensity outside the given range is clipped [16].

### 2.3 Training

We performed evaluation in 5-fold cross-validation across

The selected 888 LIDC-IDRI cases. We split 888 cases into 5

subsets and kept the number of candidates on each subset similar. For each fold, we used 3 subsets for training, 1 subset for validation, and 1 subset for testing. One of the challenges of using ConvNets is to efficiently optimize the weights of ConvNets given the training dataset. RMS Prop, a learning algorithm that adaptively divide the learning rate by a running average of the magnitudes of recent gradients, is used to optimize the model. The loss is measured by using cross-entropy error and the weights are updated using mini-batches of 128 examples. Dropout with a probability of 0.5 is implemented on the output of the first fully connected layer as regularization. Training is stopped when the accuracy on the validation dataset does not improve after 3 epochs. We initialized the weights using normalized initialization proposed by Glorot and Bengio. The biases were initialised with zero.

### 2.4 Evaluation

Two performance metrics were measured: 1) area under the ROC curve (AUC) and 2) Competition Performance Metric (CPM) [28], which measures the average sensitivity at seven operating points of the FROC curve: 1/8, 1/4, 1/2, 1, 2, 4 and 8 FPs/scan. AUC shows the performance of ConvNet's on classifying candidates as nodules or non-nodules while Cumshaw's the performance of CAD at operating points that are likely used in practice. It has to be noted that a system with higher AUC score may not necessarily result in higher CPM. We also computed the 95% confidence interval and the p-value using bootstrapping with 1,000 bootstraps. The p-value was defined as the probability of one performance measure to be lower than the other, where the performance measure was the detection sensitivity at 3.0 FPs/scan.

### 2.5 Diagnosis

Diagnosis can be made by a lung biopsy. Small biopsies obtained by core needle or bronchoscopy are commonly used for diagnosis of lung nodules. CT guided percutaneous transthoracic needle biopsies have also proven to be very helpful in the diagnosis of SPN. Several features help to distinguish benign conditions from possible lung cancer. The first parameter is the size of the lesion: the smaller, the less risk for malignant cancer. Benign causes tend to have a well-defined border, whereas lobulated lesions or those with an

irregular margin extending into the neighbouring tissue tend to be malignant.

Growth of nodules also helps determine their status (malignant, infectious, or benign) in the body which is based on the time it takes for the volume to double. The typical values are less than 20 days, less than 100 days, or more than 400 days for infection based, malignant, and benign nodules respectively. If there is a central cavity, then a thin wall points to a benign cause whereas a thick wall is associated with malignancy (especially 4 mm or less versus 16 mm or more). In lung cancer, cavitation can represent central tumour necrosis or secondary abscess formation. If the walls of an airway are visible, bronchiolar is a possibility [17].

An SPN often contains calcifications. Certain patterns of calcification are reassuring, such as the popcorn-like appearance of hamartoma. An SPN with a density below 15 Hounsfield units on computed tomography tends to be benign, whereas malignant tumors often measure more than 20 Hounsfield units. Fatty tissue inside hamartomas will have a strongly negative value on the Hounsfield scale.

The growth velocity of a lesion is also informative: very fast or very slow growing tumors are rarely malignant, in contrary to inflammatory or congenital conditions. It is therefore important to retrieve previous imaging studies to see if a lesion was presented and how fast its volume is increasing. This is more difficult for nodules smaller than 1 centimetre. Moreover, the predictive value of stable lesion over a period of 2 years has been found to be rather low and unreliable [18].

### 2.6 Treatment

When a solitary pulmonary nodule is identified, plans for further action are made based on the likelihood that the nodule could be malignant cancer. If the risk of malignancy is thought to be low, follow-up imaging (usually serial CT scans) can be planned at a later time. If the initial impression is that there is a high likelihood of cancer, then a surgical intervention (such as the Video-assisted thoracoscopic surgery) is appropriate (provided that the patient is fit for surgery). For cases in which some action is required but the situation is uncertain, guidelines exist to recommend how much surveillance there should be in defined circumstances. If a pulmonary nodule has not grown for two years and the person has no prior history of cancer then that nodule is extremely unlikely to be malignant. If the nodule is "ground glass" then longer follow up is required but the same applies. More frequent CT scans than what is recommended has not been shown to improve outcomes

but will increase radiation exposure and the unnecessary health care can be expected to make the patient anxious and uncertain [19] [20].

If there is an intermediate risk of malignancy, further imaging with positron emission tomography (PET scan) is appropriate (if available). Around 95% of patients with a malignant nodule will have an abnormal PET scan, while around 78% of patients with a benign nodule will look normal on PET (this is the test sensitivity and specificity). Thus, an abnormal PET scan will reliably pick up cancer, but several other types of will also show up on a PET scan. If the nodule has a diameter below 1 centimetre, PET scans are often avoided because there is an increased risk of falsely results. Cancerous lesions usually have a high metabolism on PET, as demonstrated by their high uptake of FDG. If the lesion is found on further imaging to be suspicious, it should be surgically excised to confirm the diagnosis by microscopically examination [20].

Other imaging techniques include PET-CT (simultaneous PET scan and CT scan with superposition of the images), magnetic resonance imaging (MRI) or single photon emission computed tomography(SPECT).

**3. EXPERIMENTAL RESULTS**

The experiments are conducted using MATLAB on the PC with Intel-Core i5 CPU 3.20GHz and 2GB of RAM without any particular code optimization.. These two databases are covering extensively, includes lung cancer, pulmonary nodule, emphysema and so on. In our study, we collected 724 cases of SPN from a total of 2664 lung DR images.

Input image

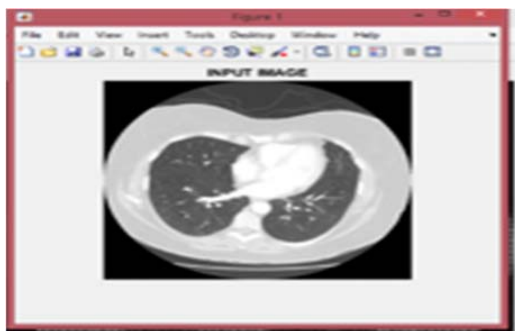


Fig 4.1.Input Image

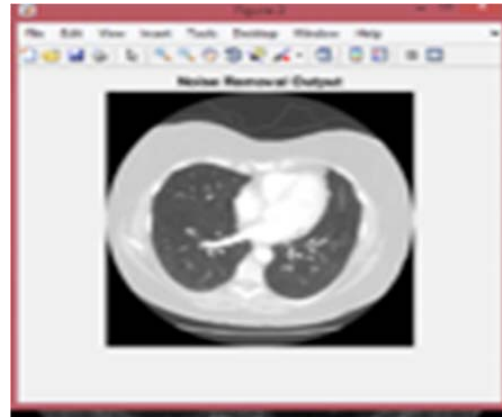


Fig 4.2 Preprocessing Image



Fig 4.3.BORDER CORRECTED OUTPUT



Fig 4.4. CLAME Equalization Output



Fig 4.7. Segemented Image

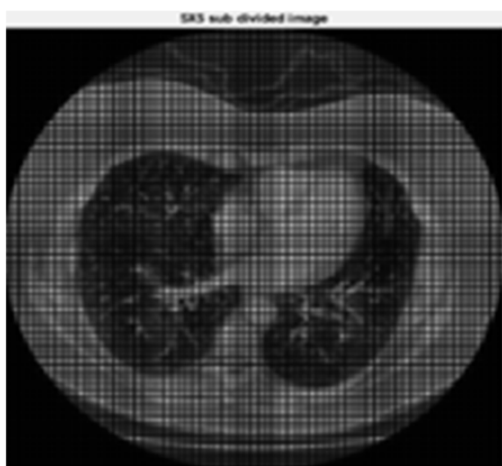


Fig 4.5 SAS Subdivide Image



Fig 4.8 Segmentation Output

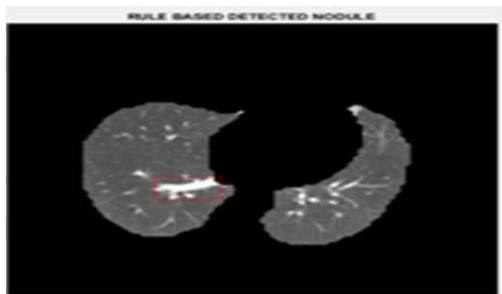


Fig 4.6. Rule Detected Module

#### 4. CONCLUSION

In order to achieve an automatic segmentation of SPN in DR images, a new image segmentation model is proposed. We have presented a system for pulmonary nodule detection in CT scans based on multi-view convolutional networks. By comparison analysis above, the proposed method have attained more accurate results and dealt inhomogeneous sub-regions. However, the CPU-time of the proposed method is higher, which caused by the times of smoothing and walking. So, in our further study, we plan to optimize parameters of smoothing and discuss the relationship between filtering

and walking techniques. The promising results and the low computation time make the ConvNets- highly suited to be used as a decision aid in a lung cancer screening scenario. Moreover, split Bergman method is effective method which could be introduced to improve the performance of the sequential filtering in the future.

## REFERENCES

- [1] Field J K, Devaraj A, Duffy S W, et al. CT screening for lung cancer: Is the evidence strong enough?[J]. *Lung Cancer*, 2016, 91: 29-35.
- [2] Rossi G, Cavazza A, Casali C, et al. Tuberos sclerosi complex presenting as a pulmonary solitary nodule[J]. *Histopathology*, 2006, 48(6): 769-771.
- [3] Nakagomi K, Shimizu A, Kobatake H, et al. Multi-shape graph cuts with neighbor prior constraints and its application to lung segmentation from a chest CT volume[J]. *Medical image analysis*, 2013, 17(1): 62-77.
- [4] Harrison R M. Digital radiography.[J]. *Physics in Medicine & Biology*, 1988, 33(7):751-84.
- [5] Kak A C, Slaney M. Principles of Computerized Tomography Imaging[J]. *Medical Physics*, 2002, 29(1).
- [6] Hatabu H, Chen Q, Stock K W, et al. Fast magnetic resonance imaging of the lung[J]. *European journal of radiology*, 1999, 29(2): 114-132.
- [7] Bley T A, Baumann T, Saueressig U, et al. Comparison of radiologist and CAD performance in the detection of CT-confirmed subtle pulmonary nodules on digital chest radiographs.[J]. *Investigative radiology*, 2008, 43(6):343-8.
- [8] Armato III S G, McLennan G, McNitt-Gray M F, et al. Lung image database consortium: Developing a resource for the medical imaging research community 1[J]. *Radiology*, 2004, 232(3): 739-748.
- [9] Lu X, Wang X, Li D, et al. Comparative study of DR and CT in the application of close contacts screening for tuberculosis outbreaks[J]. *Radiology of Infectious Diseases*, 2016, 3(1): 34-39.
- [10] Takasugi J E, Godwin J D. The Solitary Pulmonary Nodule: Radiologic Assessment[M]//*Radiologic Diagnosis of Chest Disease*. Springer London, 2001: 462-484.
- [11] Mitra S, Barman B. Rough-fuzzy clustering: an application to medical imagery[C]//*International Conference on Rough Sets and Knowledge Technology*. Springer Berlin Heidelberg, 2008: 300-307.
- [12] Bahlmann C, Li X, Okada K. Local pulmonary structure classification for computer-aided nodule detection[C]//*Medical Imaging*. International Society for Optics and Photonics, 2006: 614451-614451-11.
- [13] Yuen S Y, Ma C H. Genetic algorithm with competitive image labelling and least square[J]. *Pattern Recognition*, 2000, 33(12): 1949-1966.
- [14] Raman V, Sumari P, Then P. Matab Implementation and Results of Region Growing Segmentation Using Haralic Texture Features on Mammogram Mass Segmentation[M]//*Advances in Wireless, Mobile Networks and Applications*. Springer Berlin Heidelberg, 2011: 293-303.
- [15] Kichenassamy S, Kumar A, Olver P, et al. Gradient flows and geometric active contour models[C]// *International Conference on Computer Vision*. IEEE Computer Society, 1995:810-815.
- [16] Chan T F, Vese L A. Active contours without edges[J]. *IEEE Transactions on image processing*, 2001, 10(2): 266-277.
- [17] Grady L. Random walks for image segmentation[J]. *IEEE transactions on pattern analysis and machine intelligence*, 2006, 28(11): 1768-1783.
- [18] Qin C, Zhang G, Li G, et al. Multiclass Color-Texture Image Segmentation Based on Random Walks Framework Integrating Compact Texture Information[C]//*Proceedings of the 3rd International Conference on Multimedia Technology (ICMT 2013)*. Springer Berlin Heidelberg, 2014: 357-364.
- [19] Hao X, Shen Y, Xia S. Automatic mass segmentation on mammograms combining random walks and active contour[J]. *Journal of Zhejiang University SCIENCE C*, 2012, 13(9): 635-648.
- [20] Goshtasby A, Satter M. An adaptive window mechanism for image smoothing[J]. *Computer Vision and Image Understanding*, 2008, 111(2): 155-169.
- [21] Meyer Y. Oscillating Patterns in Image Processing and Nonlinear Evolution Equations: The Fifteenth Dean Jacqueline B. Lewis Memorial Lectures[J]. *Of University Lecture*, 2001, 22:122.

